Available online at www.sciencedirect.com
SCIENCE DIRECT®

International Journal of Pressure Vessels and Piping 82 (2005) 299–310

INTERNATIONAL JOURNAL OF
Pressure Vessels and Piping

www.elsevier.com/locate/ijpvp

Measurement of the residual stresses in a stainless steel pipe girth weld containing long and short repairs

P.J. Bouchard[a,*], D. George[b], J.R. Santisteban[c], G. Bruno[c], M. Dutta[c], L. Edwards[c], E. Kingston[b], D.J. Smith[b]

[a]British Energy Generation Ltd, Barnett Way, Barnwood, Gloucester GL4 3RS, UK
[b]Department of Mechanical Engineering, University of Bristol, Bristol BS8 1TR, UK
[c]Department of Materials Engineering, Open University, Milton Keynes MK7 6AA, UK

Abstract

A series of residual measurements were made to obtain the through-thickness residual stress profiles in an as-welded and repair welded stainless steel pipe. Long and short length repairs were manufactured after initial measurements in the original girth weld. Measurements were made using neutron diffraction, deep hole and surface hole techniques. The various measurement methods were found to complement each other well. All the measurements revealed a characteristic profile for the through-thickness distribution of the residual stresses in the heat-affected zone. The residual stresses at mid-length of the heat affected zone of the short repair were found to be higher than in the long repair.

Keywords: Deep hole drilling; Manual metal arc; Residual stress

1. Introduction

Repair welds are usually introduced into structures either to remedy initial fabrication defects found in castings or welds by routine inspection, or to rectify in-service degradation of components and thereby extend the life and economic operation of ageing engineering plant. The type of repair can range from filling a very localised shallow excavation using standard weld procedures, to welding deep excavations that can extend around a significant proportion of a structure. The latter kind of major repair may require the development of special welding procedures, for example as described by Hunter et al. [1] for nuclear power plant. Repairs can be further categorised into those centred on the original weld and those that are offset from the weld centre-line. The need to rectify lack of side-wall fusion defects, or degraded heat affected zone (HAZ) material, typically leads to offset repairs, or centred repairs encompassing material beyond the original fusion boundary.

A recent survey of weld repair technologies currently used by EPRI member utilities [2] has found that 40% of all repairs to steam chests, piping and headers resulted in subsequent cracking. It further reports that over 70% of the repairs were performed without implementing post-weld heat treatment. It is reasonable to infer that high residual stresses associated with the repair process probably played an important role in the many of these subsequent failures. The detrimental influence of residual stresses has been well documented for the case of a steam leak at a non-stress relieved pipe-work repair weld [3]. Here both the magnitude and multi-axial nature of the residual stress field was instrumental in driving creep damage leading to reheat cracking.

Accurate structural integrity assessments require a good description of the through-wall residual stress field in the component. However, reliable characterisation of residual stresses at non-stress-relieved welds is notoriously difficult. Some recommended upper bound residual stress profiles can be found in the R6 Revision 4 defect

* Corresponding author. Tel.: +44-1452-653-160; fax: +44-1452-653-025.
E-mail address: john.bouchard@british-energy.com (P.J. Bouchard).

0308-0161/$ - see front matter © 2004 Elsevier Ltd. All rights reserved.
doi:10.1016/j.ijpvp.2004.08.008

assessment procedure [4], as well as alternative structural integrity codes. Development of more realistic residual stress profiles for structural assessment requires high quality experimental measurements coupled with an understanding of component structural behaviour and non-linear analytical modelling of the welding processes responsible. Publications detailing measurements of through-wall residual stress distributions at repair welds are sparse. Leggatt [5] used block sectioning to measure transverse residual stresses associated with an extended, offset, 28 mm deep multi-pass repair weld in a 75 mm thick C–Mn steel panel, containing an original double-V weld which had been stress relieved. The same technique was applied to quantify residual stresses at extended, 50% and 67% depth, axial repairs in ferritic pressure vessels [4, 6]. Through-wall residual stresses at an extended, 35 mm deep, multi-pass repair in a 60 mm restrained ferritic thick plate containing an original double-V weld have been measured employing the deep hole (DH) technique [7], and the results compared with finite element simulations [8]. The DH method has also been applied to measure residual stresses associated with short-length, centrally embedded repairs to a 37 mm thick stainless steel girth weld [9,10]. Neutron diffraction (ND) has been used to characterise the residual stress field at a short-length, 50% depth, centrally embedded repair in a 20 mm thick, 170 mm OD stainless steel pipe [11].

2. Materials and geometry

2.1. Manufacture of test component

Residual stress measurements were carried out on a test component manufactured from two ex-service forged AISI Type 316H stainless steel steam headers provided by British Energy. The 432 mm outside diameter by 63.5 mm thick headers were bore-machined to an average thickness of 19.6 mm and then solution heat treated (for 1 h at 1050 °C followed by air cooling) to remove any residual stresses remaining from original fabrication of the headers.

One end of each header was further machined to form a J-groove girth weld preparation. The matching sections were mounted on a mandrel and joined using a ‘down-hand’ welding technique by slowly rotating the component about its horizontal axis. This minimised circumferential variations in heat input associated with the welding position. The root pass was made using the tungsten inert gas (TIG) method. Subsequent passes were made by the manual metal arc (MMA) method using Babcock ‘Type S’ electrodes of varying size conforming to BS 2926 19.12.3LBR. The final arrangement of the bored and welded headers, creating a Type 316H stainless steel pipe component is shown in Fig. 1. Further geometric parameters, material properties and weld characteristics are provided in Table 1.

After welding, one end of the test pipe was shortened by 190 mm to ensure that the large fabricated component would fit into the neutron diffractometers for strain measurements. A rectangular slot, 90 mm long around the circumference and 50 mm wide, was machined on the weld line at 345° from top dead centre (TDC). This enabled measurements in the hoop direction to be made with the neutron beam only passing once through the thickness of the pipe. No significant strain relaxation ($\pm 10\ \mu\varepsilon$) was measured using strain gauges in vicinity of the repair weld locations during this machining.

2.2. Introduction of repair welds

Following residual stress measurements on the plain girth weld, described later, two repair welds were introduced into the test component using typical manufacturing practice. A $\approx 20°$ arc-length short repair, WR1, was introduced circumferentially centred at 70° from TDC and a $\approx 62°$ arc-length long repair, WR2, centred at 240° from TDC. The locations of the repairs are shown schematically in Fig. 2. The circumferential positions of the repairs were

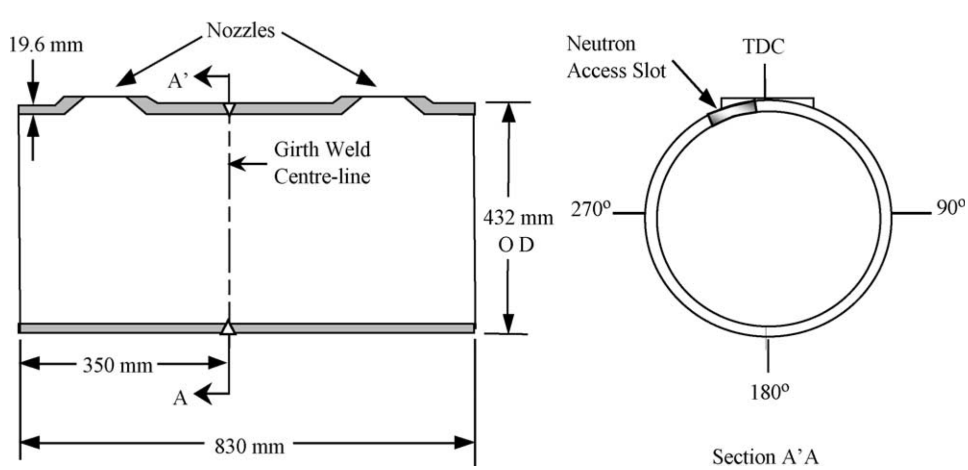

Fig. 1. Arrangement of test component.

Table 1
Summary of test component geometry and weld parameters

Component		Characteristics		
Global geometry	Outer radius, R_0 (mm)	216		
	Wall thickness, t (mm)	$\approx$19.6		
	R_m/t	10.5		
Base material	Stainless steel	AISI Type 316H		
	0.2% Proof stress (MPa)	212		
	1% Proof stress (MPa)	272		
Weld characteristics	Designation	Girth	WR1	WR2
	Weld type	MMA	MMA	MMA
	No. of passes	16	12	12
	Average arc energy (kJ/mm)	1.35	1.48	1.38
	Weld material	316L	316L	316L
	1% Proof stress (MPa)	446	446	446
Geometry of welds	Arc-length, L (degrees)	360	20	62
	Groove width (mm)	22	24	23
	Depth d (mm)	19.6	14	15
	Relative depth d/t (%)	100	71	77

carefully chosen to minimise interaction effects with each other and with the header nozzles at TDC. Repair cavities were excavated using grinding tools and rotary burrs to a depth of 71–77% of the thickness of the wall ($\approx$14–15 mm). The cavities were offset from the centre-line of the original weld by about 12 mm (see Fig. 2b). Three passes with 2.5 mm diameter MMA electrodes and nine passes of 3.2 mm diameter electrodes were used to fill each repair cavity. The welding conditions are summarised in Table 1.

3. Residual stress measurement techniques

3.1. Neutron diffraction

The ND method is a well-established method for measuring residual stresses in metallic samples, [12]. Essentially all diffraction investigations of stresses and strains are based on continuum mechanics using Hooke's law for stress calculations. The only major alteration is the use of diffraction elastic constants for specific crystallographic planes rather than the overall aggregate average. In neutron strain scanning, the elastic strain, ε, in a small gauge volume of the component is defined from the change in the lattice parameter, a, of the crystalline material referred to the unstressed value, a_0, thus $\varepsilon=(a-a_0)/a_0$. From the elastic strains, ε_{ij}, in the gauge volume measured along mutually orthogonal directions, the stress is then calculated using [13]:

$$\sigma_{ij}=\frac{E_{hkl}}{1+\nu_{hkl}}\varepsilon_{ij}+\frac{\nu_{hkl}E_{hkl}}{(1+\nu_{hkl})(1-2\nu_{hkl})}\delta_{ij}\varepsilon_{pp} \quad (1)$$

where p is a dummy suffix summing over $p=1, 2, 3$.

A variety of ND measurement facilities were used for the measurement programme and these are described later.

3.2. Deep hole drilling

The DH drilling method [7] measures the distortion of a reference hole, 3.175 mm diameter, drilled through

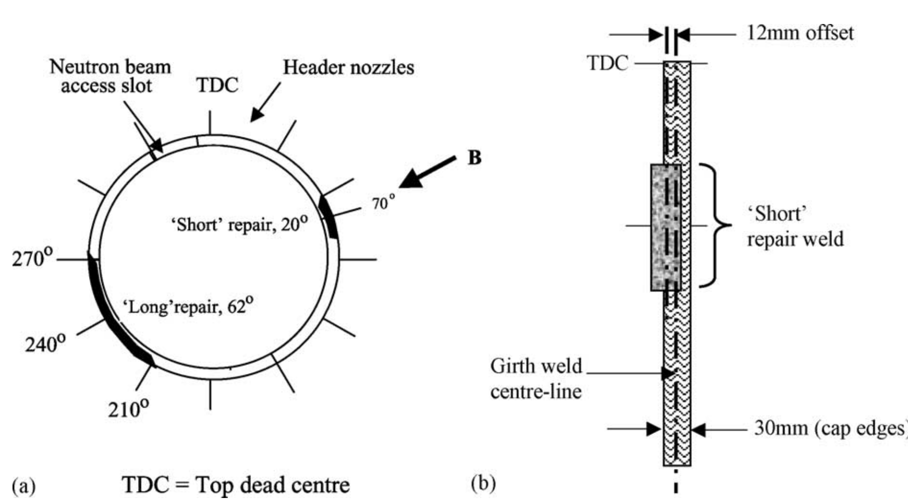

Fig. 2. (a) Section A′A (see Fig. 1) showing circumferential positions of short and long weld repairs, (b) view on B of short repair showing offset.

the component. Prior to drilling the reference hole, small steel bushes are glued to the surfaces of the component. The reference hole is drilled through the component and the bushes. Accurate measurement of the diameter of the reference hole is made through the thickness at different angles around the circumference. Then a column of material containing the reference hole as its axis is trepanned free of the component, which allows the residual stresses in the core to be relaxed. The differences in diameters before and after trepanning provide strain information for subsequent analysis to determine residual stresses. It is assumed that the reference hole lies along a maximum principal stress direction. The standard method, originally developed for heavy section components, uses a 20 mm diameter core giving stresses averaged over about an 8 mm diameter gauge area. The accuracy of the technique has been determined to be ± 30 MPa in stainless steel [10]. More recently the technique has been applied to thinner structures using a 10 mm diameter core having a smaller effective gauge area.

4. Measurements and results

The various measurements performed using the ND and DH drilling methods are summarised in Table 2. First, a series of ND measurements were made in the girth weld at two positions at 7 and 14 mm to one side of the weld centre-line. This is shown in Fig. 3a. The ND measurements were followed by a series of DH measurements at three locations around the circumference of the girth weld.

After the manufacture of the repair welds further sets of ND and DH measurements were made adjacent to the short, WR1, and long, WR2, repairs. The through-thickness locations are shown in Fig. 3b.

The ND measurements were carried out at two instruments. For the girth weld and the long repair, WR2, weld measurements were performed using the REST instrument of the NFL (Laboratory for Neutron Scattering) in Studsvik (Sweden). The (311) reflection was chosen for the measurements as this is known to be insensitive to elastic and plastic anisotropy effects in stainless steel [14]. The scattering angle was $\approx 108.6°$ for the chosen (311) peak at the selected wavelength of ≈ 1.76 Å.

For the short repair, WR1, weld ND measurements were performed on the ENGIN spectrometer at the ISIS pulsed neutron source, UK [15].

In order to calculate strains and hence stresses from ND measurements the stress free lattice parameter for the materials being studied must be known. Furthermore, if there is any change in chemical composition or heat treatment over the area being studied, then any effects on stress free lattice parameter must also be characterised. This component was manufactured from two different ex-service steam header forgings produced from two different material casts. This means that although both materials were solution treated prior to welding, the stress free lattice parameters for these two parent materials were likely to differ as the stress free lattice parameter of stainless steel is very sensitive to the amount of carbon and nitrogen in solution [16]. In addition, differences in stress free lattice parameter may occur due to local heat treatment of the parent metal and HAZ during the welding process.

The usual way to deal with this problem is to machine small stress-relaxed cubes from the weld and surrounding material and measure their lattice parameter. However, this necessarily involves cutting up the specimen and so relieving the very stresses you are trying to measure. Hence, a novel two pronged strategy was adopted in this work to minimise removing material from the specimen whilst still obtaining the stress free lattice parameter variation both across the weld and between the two forgings.

First, the 20 mm diameter DH core, DH1, which sampled parts of the original girth weld, as well as HAZ and adjacent parent material from one header was cut into small 3 mm cubes in order to establish the stress free lattice parameter variation that occurs due to welding. These measurements were undertaken on the REST instrument at NFL Studsvig. Second, the HAZ and parent material taken from this sample were compared with parent material obtained when one end of the test pipe was shortened by 190 mm to ensure that it would fit into the neutron diffractometers and also with HAZ material from the 10 mm DH core DH4 taken from the second header. This comparison was undertaken on

Table 2
Summary of measurements locations

Weld	Measurement method	Distance from girth weld centre-line (mm)	Angle from TDC (degrees)
Girth weld	Neutron diffraction	−14, −7	270
	Deep hole, DH1 (20 mm core)	15	120
	Deep hole, DH2 (20 mm core)	−13	150
	Deep hole, DH3 (10 mm core)	−13	100
Short repair WR1 (20° arc-length)	Neutron diffraction	−24	70
	Deep hole, DH4 (10 mm core)	−24	70
Long repair WR2 (62° arc-length)	Neutron diffraction	−24	270
	Deep hole, DH5 (10 mm core)	−24	240

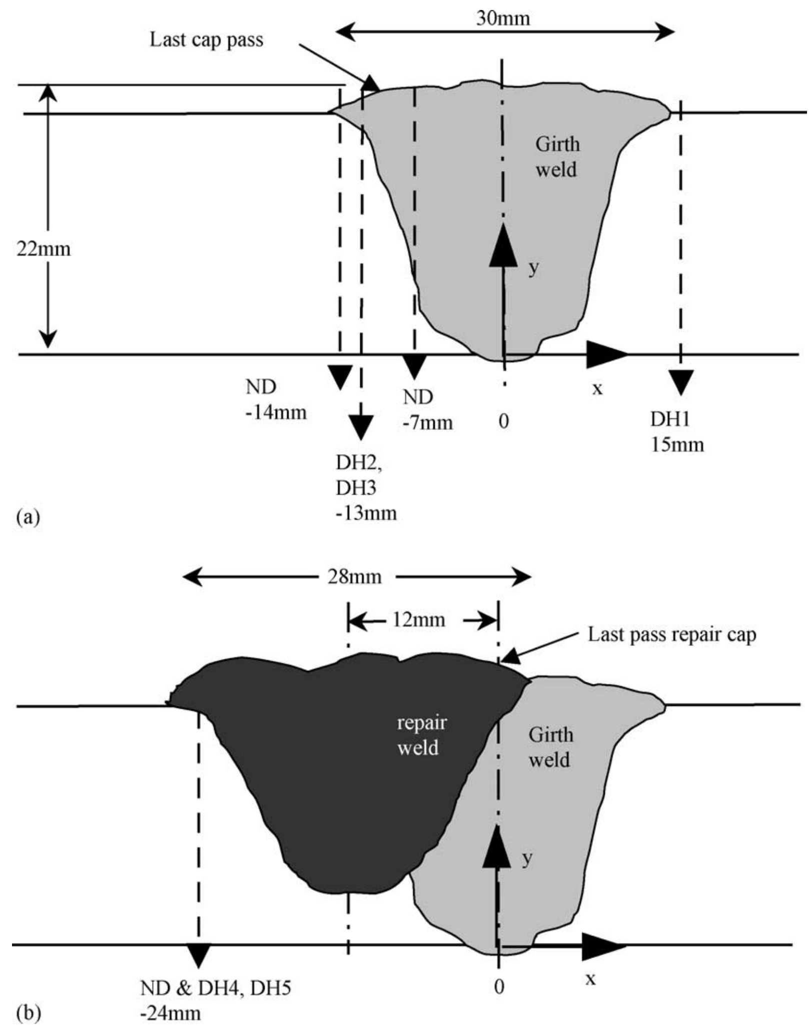

Fig. 3. Positions of neutron diffraction and deep hole measurements: (a) in girth weld and (b) repair welds.

the ENGIN instrument at ISIS, where the short repair measurements were made.

All DH measurements were carried out at Bristol University laboratories using a standardised procedure [9].

4.1. Girth weld

For the ND measurements at NFL Studsvik, the pipe was positioned upright for the hoop measurements and horizontal for the other two directions. For measurements of hoop strain, it was arranged for the incoming neutron beam to pass through the access slot with the primary slit placed inside the pipe. The width of the primary slit was maintained at 3 mm for all measurements; but the height was adjusted to 3 mm for the hoop direction and small reference cubes (for stress-free lattice plane, d_0 measurements); 5 mm for the axial direction; and 10 mm for the radial measurements. The gauge volume was always kept completely immersed in the material.

As noted above, the stress free reference lattice parameter, a_0, across the weld was determined from neutron measurements of the (311) lattice plane spacing (d_0) in small $3\times3\times3$ mm^3 cubes taken from the weld pool, the HAZ and the parent material. Cubes from each region were scanned in axial and hoop directions The average a_0 values were found to be very similar in both the parent material and the HAZ (3.5965 ± 0.0001 Å), as previously seen in a Type 316 weld [11,17]. No significant variation in the lattice parameter through the thickness of the HAZ was found. However, higher scatter was found in the average values in the weld pool (3.5955 ± 0.0003 Å). Based on these findings, a constant value of a_0 of 3.5965 ± 0.0001 Å was used for HAZ and parent material.

DH measurements DH1 and DH2 were made in the girth weld HAZs of the two headers using a standard 20 mm diameter core. The lack of detail in the measured stress distributions, when compared with the ND measurements, prompted a further measurement in the HAZ using a smaller 10 mm diameter core.

The measured axial and hoop residual stresses from the ND and DH measurements are compared in Fig. 4 together with some additional surface hole measurements. Fig. 5

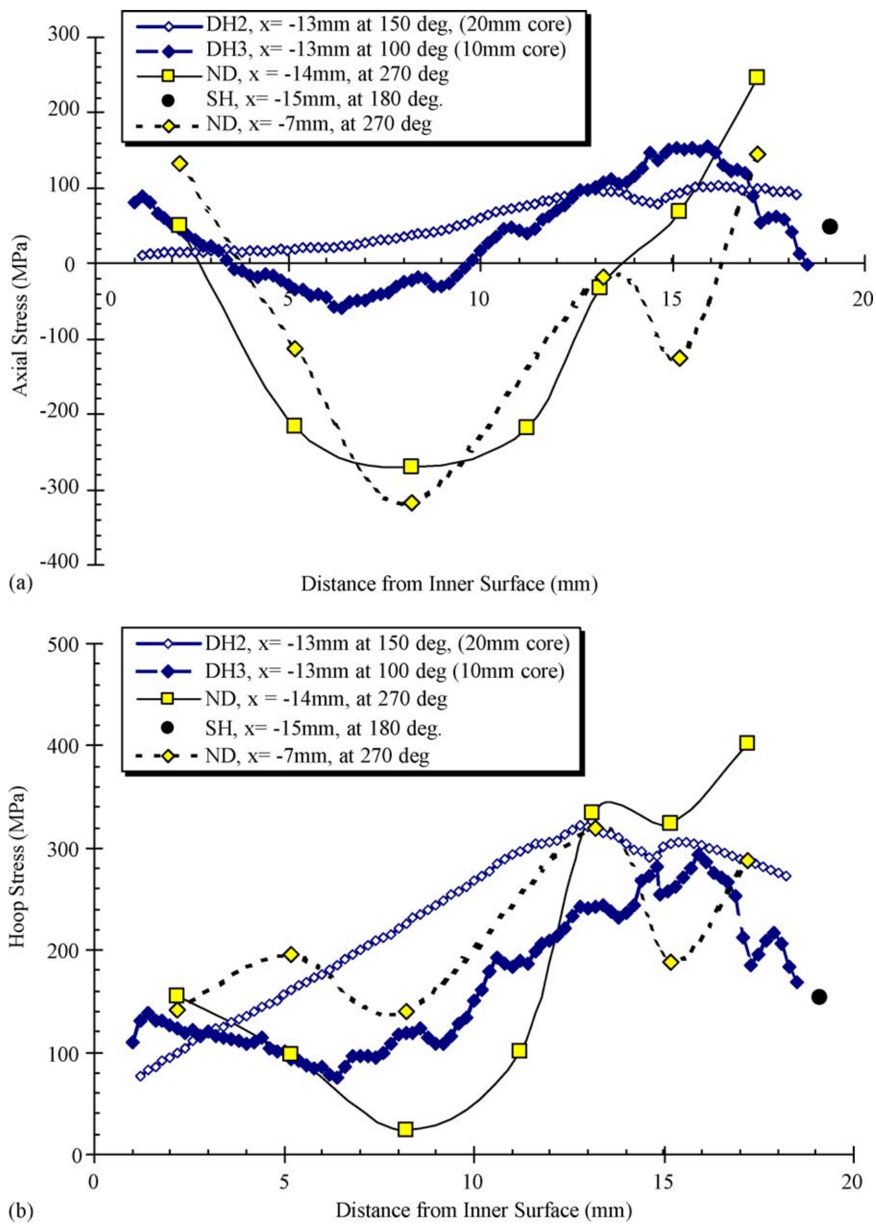

Fig. 4. Comparison of measured residual stresses in the HAZ of the original girth weld under the last weld cap pass ($x = -7$ to -15 mm) at various angles from TDC: (a) axial (b) hoop.

shows axial and hoop residual stresses from the three DH measurements. For the measurements under the last pass of the weld it is evident that the 10 mm core measurement is more sensitive than the 20 mm core, resolving a far more detailed stress distribution through the wall. Nonetheless, the 20 mm diameter core results clearly indicate that stress distributions in the HAZs on either side of the girth weld significantly differ from each other.

4.2. Repair welds

For ND measurements on the short repair weld at the ENGIN spectrometer (ISIS) the strains in the hoop, radial and axial directions were measured using a gauge volume size of $5 \times 1.7 \times 3$ mm^3. The lattice parameters were obtained by Rietveld refinement of the whole diffraction spectra using the GSAS code [18]. A fibre texture (March–Dollase) model was adopted to account for preferred orientation observed in three sample positions close to the outer surface. For the outermost position, where the gauge volume was only partially embedded in the specimen, the measured strains were corrected using the method described in [19]. As many reflections (and hence many crystal orientations) are involved in the definition of the measured lattice parameter, the macroscopic values of Young's modulus and Poisson's ratio ($E = 195.6$ GPa, $\nu = 0.294$) were adopted in the analysis to derive stresses.

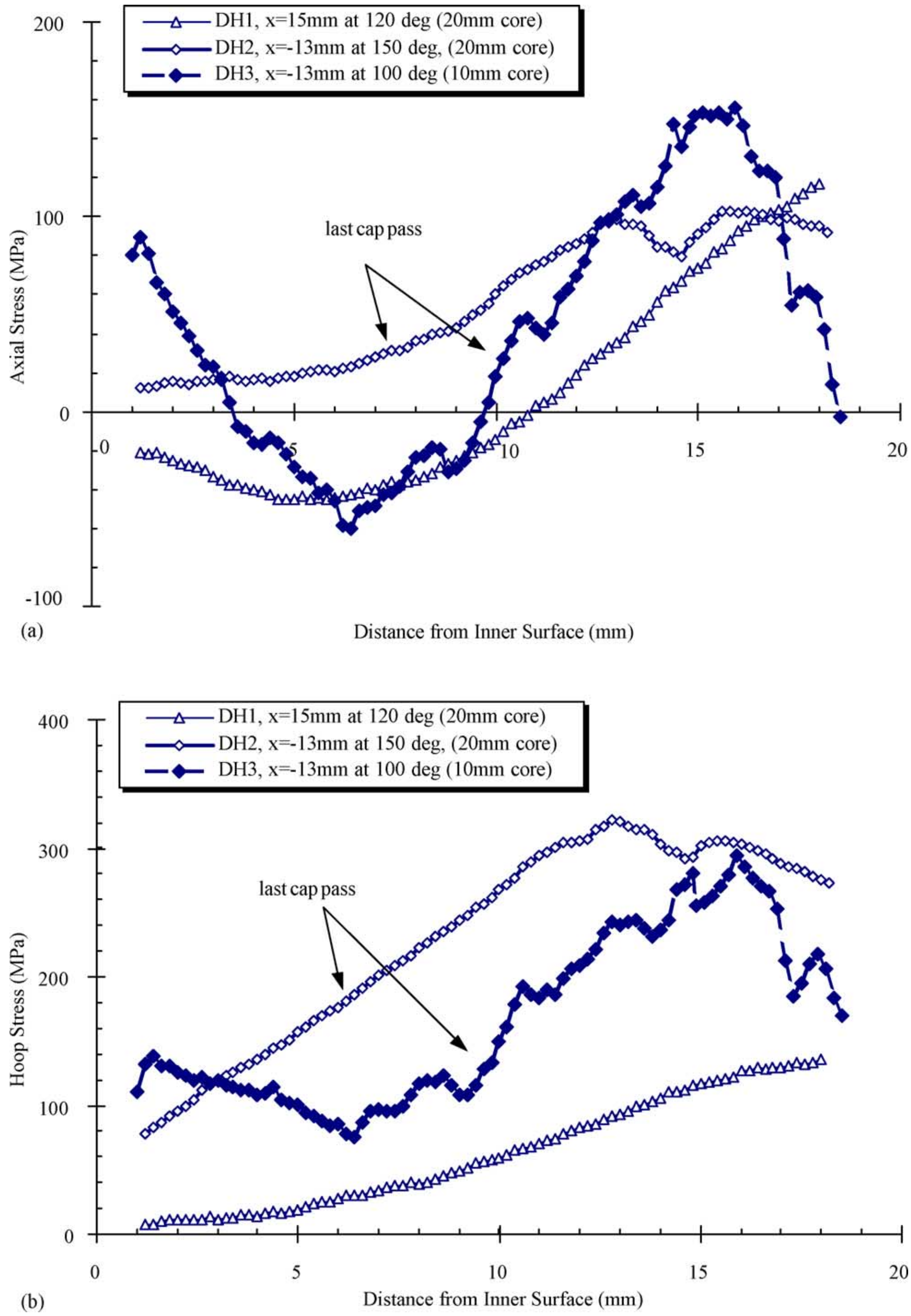

Fig. 5. Deep hole residual stress measurements in the HAZ of the original girth weld: (a) axial, (b) hoop.

The second set of stress free lattice parameter measurements were performed on the ENGIN spectrometer using the Bragg edge transmission technique [20] at the ISIS pulsed neutron source, UK [15]. Measurements were carried out on the parent material and HAZ cubes from DH1 measured at Studsvig, plus specimens produced from the second header parent material and HAZ as described above. It was found that there was a difference in measured a_0 values between the two header HAZs equivalent to a strain difference of $310 \pm 50\ \mu\varepsilon$. A negligible difference (equivalent to a strain of $60 \pm 50\ \mu\varepsilon$) was found between the measured a_0 values of the original girth weld HAZ and repair weld HAZ in the same header. From these measurements appropriate values of the unstressed lattice parameter a_0 (or lattice plane spacing d_0) were applied to each header HAZ material, that is 3.5965 ± 0.0001 Å for the repair weld side of the pipe (which had been shortened by 190 mm as

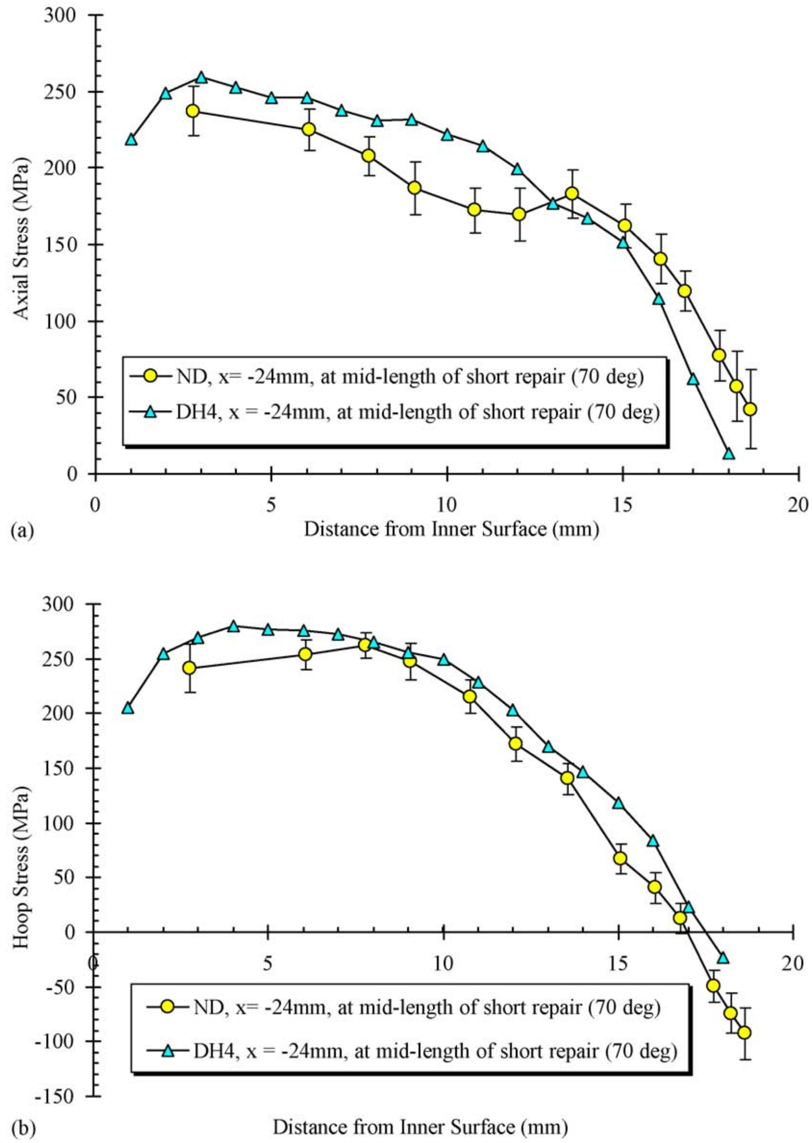

Fig. 6. Comparison of measured residual stresses at mid-length of the short repair weld HAZ ($x = -24$ mm) at 70° from TDC: (a) axial, (b) hoop.

noted above) and 3.596854629 ± 0.0001 Å for the girth weld side of the pipe.

For the long repair weld, ND measurements were made at NFL Studvisk using the same procedure as for the girth weld described earlier. ND measurements were carried out to characterise the distribution of through-wall residual strains and stresses in the HAZ adjacent to the long (62° arc-length) repair weld. A circumferential position at the end of the repair (270° from TDC) was chosen. This end corresponds to where the weld torch stopped in each repair pass. Note that the circumferential point at which the excavation has reached full depth defined the 'end' of the repair. The axial location of the measurements is the same as indicated in Fig. 3 for the short repair.

A DH drilling measurement, DH4, was performed *a posteriori* at exactly the same location as the ND measurement in the short repair [9]. A further DH measurement, DH5, was performed in the HAZ in the same axial plane (-24 mm) as the neutron measurements (Fig. 3b), but at 240 °C from TDC, that is at mid-length of the long repair. The more sensitive 10 mm diameter core was used to increase the likelihood of capturing through-wall stress gradients.

The measured axial and hoop residual stresses are shown in Fig. 6 for the short weld repair. There is an excellent correlation between the measured stresses from the ND and DH techniques. Fig. 7 illustrates the measured DH residual stresses for the long weld repair, which also show the ND results for the weld torch stop-end of the long repair. The measured stresses at the two locations show similar through wall profiles, but the end of the repair stress magnitudes are ≈ 100 MPa lower.

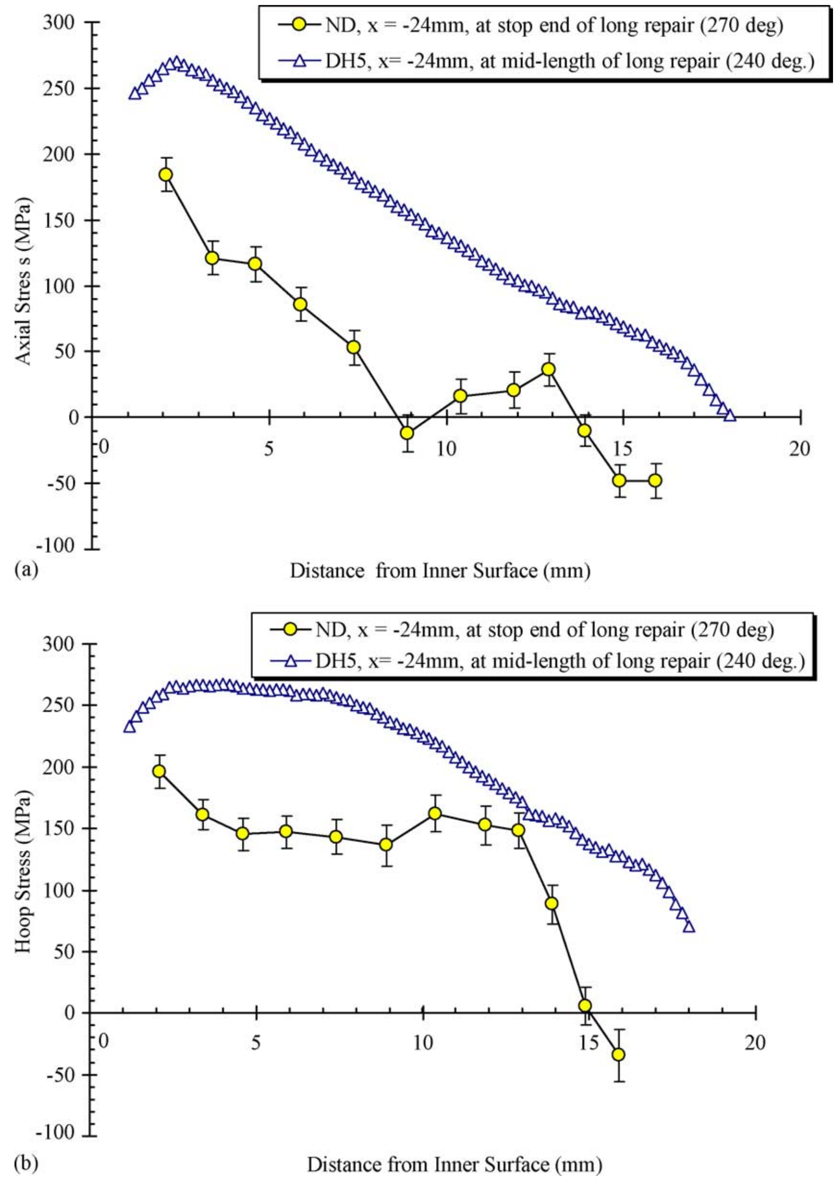

Fig. 7. Comparison of measured residual stresses at the end (270° from TDC) and mid-length (240° from TDC) of the long repair weld HAZ ($x = -24$ mm): (a) axial, (b) hoop.

5. Discussion

In the original girth weld various measurements were made beneath the last capping pass of the girth weld. The detailed through-wall profiles from ND, DH and surface centre-hole residual stress measurements in the HAZ between $x = -7$ and -15 mm are shown in Fig. 4. The more sensitive 10 mm core DH measurement (DH3) picks up the underlying axial stress profile at $x = -13$ mm revealed by the ND measurements. Both the surface hole, SH, and DH measurements show that the axial and hoop stresses fall towards the outer surface, where neutron measurements were not made. The ND measured stresses in the weld metal ($x = -7$ mm) are similar to the HAZ ($x = -14$ mm) neutron profiles, bearing in mind expected local variations owing to the individual weld beads. This gives confidence in the weld ND measurements.

Although using a 20 mm core for DH measurements is not as sensitive as using a 10 mm core, the measurements in the original HAZ of the girth weld, shown in Fig. 5 reveal that the residual stresses below the last and first pass welds differ. This evidence is supported by finite element weld simulation studies showing that the weld pass sequence, and in particular the position of the final capping pass, have a major effect on the through-wall stress distribution in this thickness of pipe, [11].

Through-wall HAZ residual stresses, shown in Fig. 8, at mid-length of the short repair (ND and DH measurements at 70°) are compared with the DH measurements at mid-length of the long repair (240°) and ND measurements

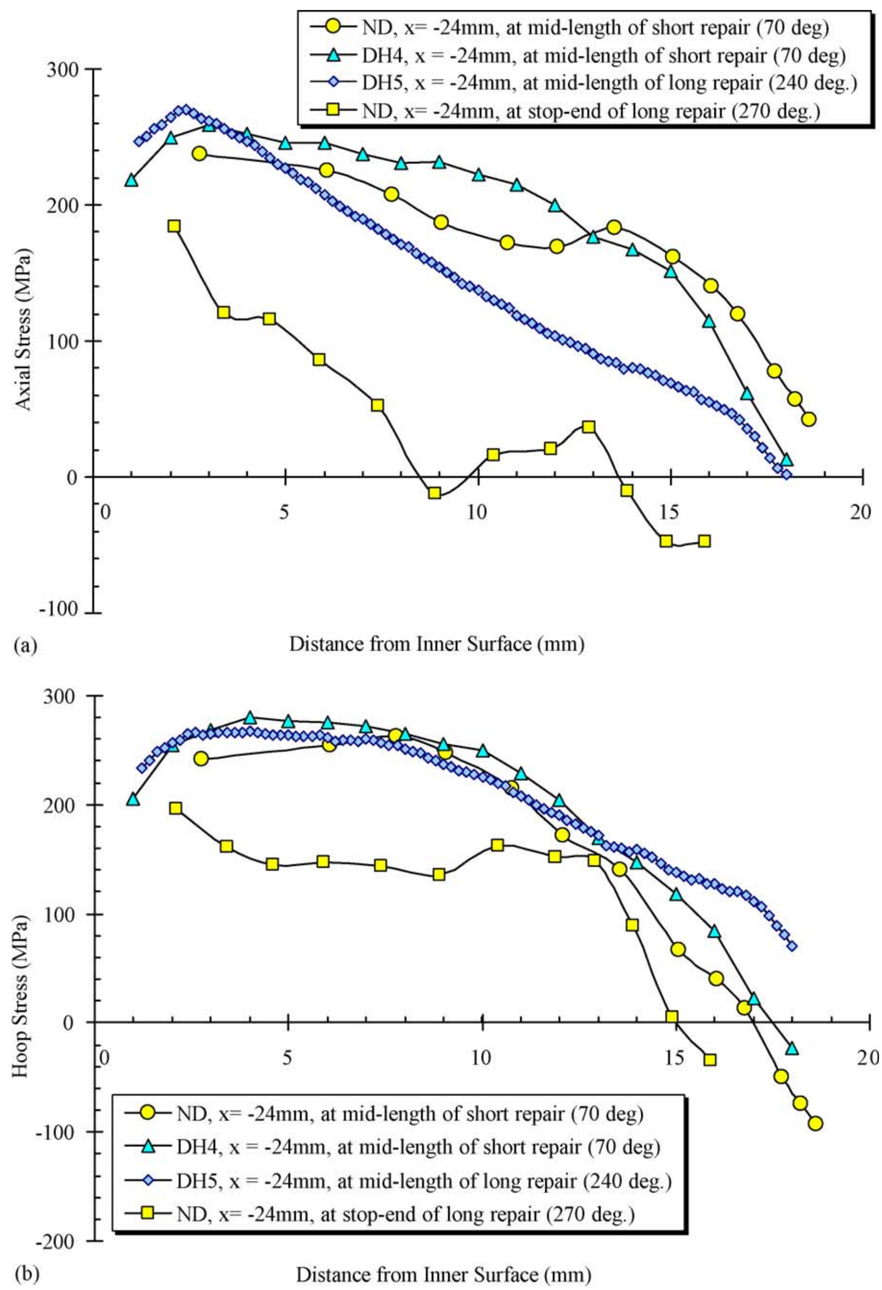

Fig. 8. Comparison of measured residual stresses through the HAZs of the short and long repair welds ($x = -24$ mm, 70, 240 and 270° from TDC: (a) axial, (b) hoop.

at the stop-end of the long repair (270°). All the measurements confirm a characteristic shape for axial and hoop through-wall profiles; namely high bi-axial tension (approximately equivalent to the 1% parent proof stress peak magnitude) towards the inner surface falling to small or compressive values towards the outer surface. The hoop stress profiles of the short and long repairs are almost identical at mid-length. Likewise the axial stress profiles at mid-length are similar to each other. However, the magnitudes of hoop and axial stresses at the end of the long repair are much lower than the corresponding stresses at mid-length. This evidence suggests that through-wall residual stresses are lower at the end of multi-pass repairs (with chamfered weld grooves) than at mid-length.

The repair weld through-wall residual stress profiles are compared in Fig. 9 with measurements judged to provide a best estimate of the original girth weld distribution. It is seen that repair welds completely change the through-wall axial and hoop residual stress profiles. The axial stresses suffer the greatest change, with a reversal from compressive yield to tensile yield at mid-thickness. It is notable that the repair weld axial stress profiles integrate through the thickness to give a net axial membrane force, confirming previous observations on a similar repair weld [11]. It is conceivable that the order of

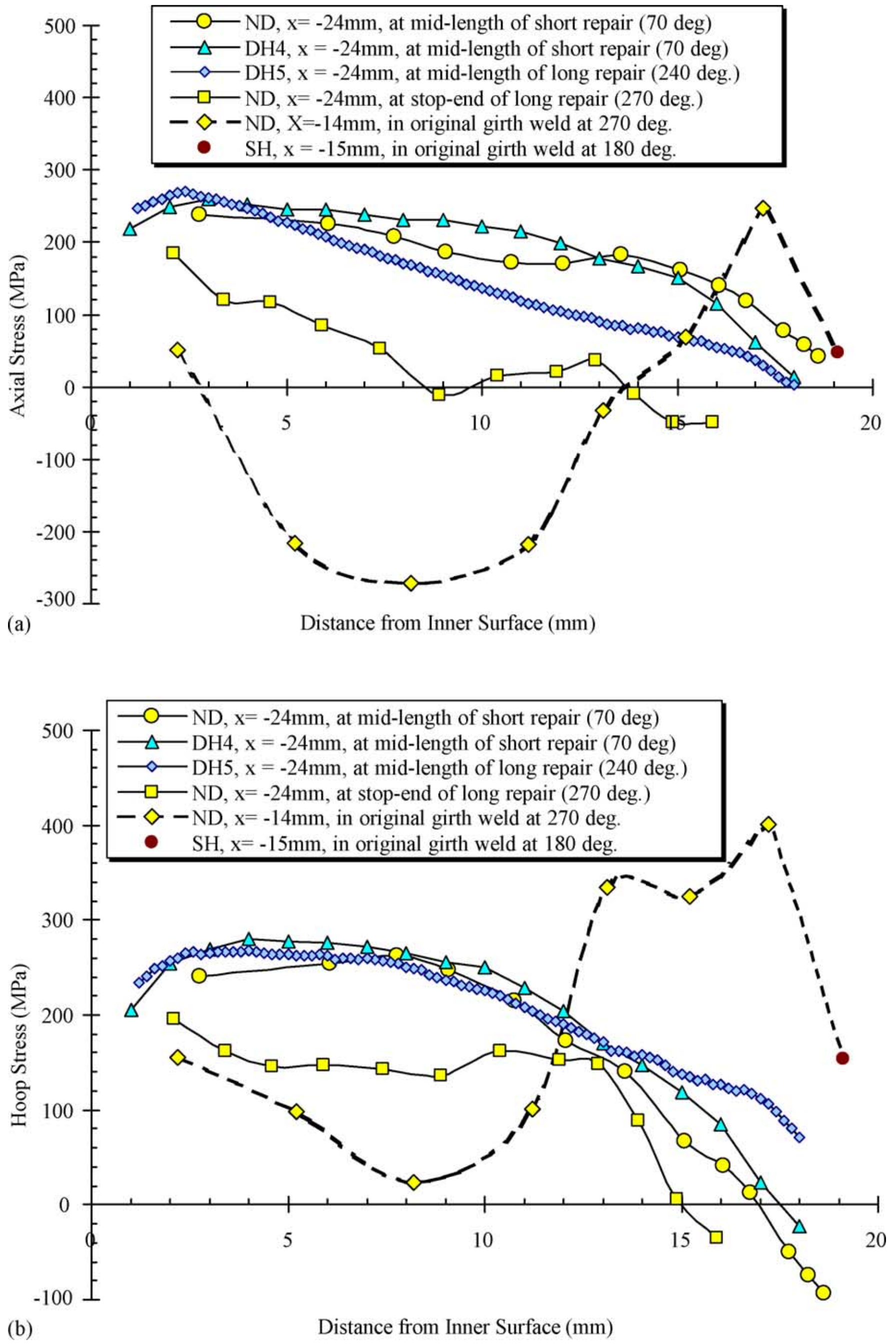

Fig. 9. Comparison of measured residual stresses through the HAZs of the short and long repair welds with the girth weld measurements: (a) axial, (b) hoop.

welding the repairs has had some influence on the resulting residual stress field. The fabrication records show that the short repair was made after the long repair. A key feature characterising repair welds is the development of high magnitude tensile membrane residual stress transverse to the welding direction as revealed by the present measurements and observed elsewhere, for example see [9,11,21,22]. Finite element studies suggest that this tensile membrane stress has a long transverse range of influence and extends along the length of a repair, see [22]. The stress is primarily induced by axial mismatch strains arising from weld filler metal contraction, which is accommodated by a combination of plastic straining of the repair weld metal and local parent material with elastic deformation of the rest of the structure. In a pipe, the transverse tensile membrane residual stress acting over the length of a part-circumference repair, must be self- balanced by compressive stresses distributed around the remaining circumference. If the average measured tensile membrane stress of 189 MPa (assumed to be acting along the length of the short repair) were reacted by a uniform compressive stress around the remaining circumference, this would only apply a compressive membrane stress of about 10 MPa at the long repair measurement locations.

6. Conclusions

Repairs to an original MMA J-preparation girth weld in a stainless steel pipe (412 mm outer diameter, 19.6 mm thick), have been examined. Two repairs were introduced, of 20 and 62° arc-length, on opposite sides of the pipe. Both repairs were axially offset from the original girth weld centre-line. The repair weld residual stress measurements mainly relate to a cross-section through HAZ material beneath the edge of the repair weld cap (that is on the opposite side of the repair from the remnant original weld). All the measurements identified a characteristic shape for axial and hoop through-wall residual stress profiles in the HAZ adjacent to the repairs; namely high bi-axial tension towards the inner surface falling to small or compressive values towards the outer surface. The measured through-wall distribution of axial residual stress in the HAZ at mid-length of the long repair was found to be lower than at mid-length of the short repair. Also the measured through-wall axial and hoop residual stresses were significantly lower at the stop-end of the long repair than at mid-length. Finally, the residual stress measurements at the short and long repairs support the theoretical expectation that repairs lead to axial through-wall stress distributions, adjacent to the repair, having high membrane content.

Acknowledgements

There were many contributions to the work presented in this paper. Staff at British Energy involved in the manufacture of the test component included Keith Abbott and Andy Wilby. The neutron diffraction measurements were carried out under Task 16 of the EU Thematic Network TRAINSS (Training Industry in Neutron Strain Scanning), EU contract BRRT-CT97-5043. Task partners were, British Energy, The Open University (UK), Tecnatom (Spain), Instituto de Soldadura e Qualidade (ISQ, Portugal), NFL (Stusdvik, Sweden), and the Rutherford Appleton Laboratory (UK). The deep hole measurements at Bristol University were supported by funding from the Industrial Management Committee [HSE(NII), British Energy and BNFL]. This paper is published with permission of British Energy Generation Limited.

References

[1] Hunter ANR, Bell WM, McDonald EJ, Specification, development, and optimisation of the welding and post-weld heat treatment procedures. In: Boiler Shell Weld Repair Sizewell A Nuclear Power Station, I. Mech. E. Seminar Publication 1999–14. London: Prof. Eng. Publishing; 1999, pp. 33–53.

[2] Gandy DW, Findlan SJ, Viswanathan R. Weld repair of steam turbine casings and piping-an industry survey. Trans ASME. J Press Vessel Technol 2001;123:157–60.

[3] Dunn J, MacGuigan J, McLean RJ, Miles L, Stevens RA. Investigation and repair of a leak at a high temperature stainless steel butt weld. Proceedings of international conference on integrity of high temperature welds. London: PEP Ltd; 1998 pp. 241–58.

[4] British Energy. Assessment of the Integrity of Structures Containing Defects. Procedure R6 Revision 4. British Energy Generation Ltd; 2003.

[5] Leggatt RH. Computer modelling of transverse residual stresses in repair welds. Weld Res Suppl 1991;70(11):299s–310s.

[6] Knee N. Coping with residual stresses in the integrity assessment of an as-welded repair. National Power (Thermal) Report ESTD/L/0111/R89, 1999.

[7] Smith DJ, Bouchard PJ, George D. Measurement and prediction of residual stresses in thick section steel welds. J Strain Anal 2000;35: 287–305.

[8] Dong P, Zhang J, Hong JK, Bell W, McDonald EJ. Finite element and experimental study of residual stresses in a multi-pass repair weld. WRC Bull 2000;455.

[9] George DBF, Determination of residual stresses in large section stainless steel welds. PhD Thesis, University of Bristol, 2000.

[10] George D, Bouchard PJ, Smith DJ. Evaluation of through wall residual stresses in stainless steel weld repairs. Mater Sci Forum 2000; 347–349:646–51.

[11] Edwards L, Bouchard PJ, Dutta M, Fitzpatrick ME. Direct measurement of residual stresses at a repair weld in an austenitic steel tube. Proceedings of the international conference on integrity of high temperature welds. London: PEP Ltd; 1998 pp. 181–91.

[12] Withers PJ, Webster PJ. Neutron and synchrotron X-ray strain scanning. Strain 2001;37(1):19–33.

[13] Noyan IC, Cohen JB. Residual Stress. New York: Springer; 1986.

[14] Daymond MR, Bourke MA, Von Dreele RB, Clausen B, Lorentzen T. Use of Rietveld refinement for elastic macrostrain determination and for evaluation of plastic strain history from diffraction spectra. J Appl Phys 1997;82:1554–62.

[15] Johnson MW, Edwards L, Withers PJ. ENGIN: a new instrument for engineers. Physica 1997;B234:1141–3.

[16] Priesmeyer HG, The stress-free reference sample: alloy composition information from neutron capture. Proceedings of NATO advance research. Workshop on measurement of residual and applied stress using neutron diffraction. Oxford: NATO ASI Series, 1992, pp. 277–84.

[17] Hutchings MT, Withers PJ, Bouchard PJ. Characterisation of the residual stress state in a double 'V' stainless steel cylindrical weldment using neutron diffraction and finite element simulation Proceedings of ICRS-6 2000 pp. 1333–40.

[18] Von Dreele RB, Jorgensen JD, Windsor CG. Rietveld refinement with spallation neutron powder diffraction data. J Appl Crystallogr 1982; 15:581–9.

[19] Wang DQ, Edwards L. Precise determination of specimen surface position during sub-surface strain scanning by neutron diffraction. Denis S, et al, editor. Proceedings of the fourth European conference on residual stresses. Société Française de Métallurgie et de Matériaux 1998;1:135–44.

[20] Santisteban JR, Edwards L, Steuwer A, Withers PJ. Mapping of unstressed lattice parameters using Bragg edge neutron transmission. J Appl Crystall 2001;34:289–97.

[21] Masubuchi K. Analysis of Welded Structures. New York: Pergamon Press; 1980.

[22] Dong P, Zhang J, Bouchard PJ. Effects of repair weld length on residual stress distribution. Trans ASME J Press Vessel Technol 2002; 124(1):74–80.